

Received March 17, 2019, accepted April 1, 2019, date of publication April 4, 2019, date of current version April 16, 2019.

Digital Object Identifier 10.1109/ACCESS.2019.2909300

Application of Parameter Optimized Variational Mode Decomposition Method in Fault Diagnosis of Gearbox

ZHIJIAN WANG^{1,2}, GAOFENG HE¹, WENHUA DU¹, JIE ZHOU¹, XIAOFENG HAN¹, JINGTAI WANG¹, HUIHUI HE¹, XIAOMING GUO¹, JUNYUAN WANG¹, AND YANFEI KOU¹

¹College of Mechanical Engineering, North University of China, Taiyuan 030051, China

²College of Mechanical Engineering, Xi'an Jiaotong University, Xi'an 030619, China

Corresponding author: Junyuan Wang (wangyi01161013@163.com)

This work was supported in part by the Shanxi Provincial Natural Science Foundation of China under Grant 201801D121186, Grant 201801D221237, Grant 201801D121187, and Grant 201601D102035, in part by the Science Foundation of North University of China under Grant XJJ201802 and Grant 2017004, and in part by the Science and Technology Innovation Project of Shanxi Province University under Grant 201802073.

ABSTRACT The selection of variational mode decomposition (VMD) parameters usually adopts the empirical method, trial-and-error method, or single-objective optimization method. The above-mentioned method cannot achieve the global optimal effect. Therefore, a multi-objective particle swarm optimization (MOPSO) algorithm is proposed to optimize the parameters of VMD, and it is applied to the composite fault diagnosis of the gearbox. The specific steps are: first, symbol dynamic entropy (SDE) can effectively remove background noise, and use state mode probability and state transition to preserve fault information. Power spectral entropy (PSE) reflects the complexity of signal frequency composition. Therefore, the SDE and PSE are selected as fitness functions and then the Pareto frontier optimal solution set is obtained by the MOPSO algorithm. Finally, the optimal combination of VMD parameters (k, α) is obtained by normalization. The improved VMD is used to analyze the simulation signal and gearbox fault signal. The effectiveness of the proposed method is verified by comparing with the ensemble empirical mode decomposition (EEMD).

INDEX TERMS Variational mode decomposition, multi-objective particle swarm, symbol dynamic entropy, power spectral entropy, fault diagnosis of the gearbox.

I. INTRODUCTION

Over the years, through the continuous exploration of many domestic and foreign scientific research workers, the reliability and accuracy [1]–[4] of fault diagnosis have been improved.

In 2014, Dragomiretskiy and Zosso [5] proposed a new adaptive fault diagnosis method, variational mode decomposition (VMD). The VMD method has the advantages of solid theoretical basis, fast convergence speed and obvious decomposition results. As a decomposition algorithm, VMD is similar to empirical mode decomposition [6] (EMD) and EEMD [7]. The fault signal can be decomposed into several intrinsic mode functions [8] (IMF) according to high and low frequencies. However, before the decomposition of the fault

signal, VMD needs to determine the decomposition number of the intrinsic mode function k and the penalty factor α in advance [9]. The decomposition number k has a great influence on the decomposition results, that is, when the k value is set too high, it will lead to over-decomposition and decompose the abnormal white noise components. However, when the k value is too low, under-decomposition will occur. The penalty factor α directly affects decomposition accuracy. The larger the value of α , the wider the bandwidth of the k modal functions obtained. On the contrary, the smaller the value of α , the smaller the bandwidth of the k modal functions obtained, thus affecting the decomposition accuracy. And if the value of k and α are improper, modal aliasing will occur. If the appropriate value is taken, the phenomenon of modal aliasing can be effectively suppressed, and the fault characteristics can be effectively extracted [10]–[13]. Therefore, the selection of the appropriate combination of parameters

The associate editor coordinating the review of this manuscript and approving it for publication was Prakasam Periasamy.

(k, α) is the key to the signal decomposition of VMD. Due to the rapid development of intelligent algorithms in recent years, such as: genetic algorithms, neural network algorithms [14]. For adaptively determining the number of modal decompositions k and the penalty factor α in the VMD, Zhang *et al.* [15] used the grasshopper optimization algorithm (GOA) to optimize the VMD parameters. In this method, first, a measurement index called a weighted kurtosis index is constructed using a kurtosis index and a correlation coefficient. Then, using the maximum weighted kurtosis as the fitness function, the VMD parameters are optimized by the GOA algorithm; Wang *et al.* [16] used the permutation entropy optimization method to adaptively determine the number of modal decompositions k ; Miao *et al.* [17] established the kurtosis of indicator set as the objective function, and optimized the objective function by using the GOA, adaptive determination values of k and α by using the GOA; Other scholars use the Ant Colony Algorithm (ACA) [18], Artificial Fish Swarm Algorithm (AFSA) [19] and other optimization algorithms to optimize parameters. Compared with the individual experience to determine the value of k and the value of α , these optimization algorithms can automatically determine the k value and the α value according to the original signal, and have well adaptability. At the same time, exclude the influence of human factors on the decomposition result. However, these methods are all constructing single objective functions for optimization, and the single objective optimization problem only considers the optimal problem in a certain sense context. Multi-objective optimization considers the optimality of multiple objective in a certain sense and it can achieve global optimal characteristics. Therefore, this paper the construction of multi-objective functions for VMD parameter optimization has certain feasibility [20].

Multi-objective Particle Swarm Optimization (MOPSO) [21]–[23] algorithm can optimize the problem by using multiple objective function indexes. Due to its simple principle and mechanism, rapid convergence speed and well global search performance, it has been successfully applied to many problems in many fields. Particle swarm optimization algorithm is an evolutionary algorithm with the advantages of simple form, rapid convergence and flexible parameter adjustment mechanism, and has been successfully applied to the single-objective optimization problem, which is considered as one of the most promising methods for solving multi-objective optimization problems [24]. And domestic and foreign scholars have done a lot of research on the improvement of this method. Shu-Kai *et al.* [25] proposed a multi-objective solution method based on particle swarm optimization, which combines multiple search strategies and empirical mobility strategies based on the Pareto advantage concept. The results show that there are great advantages for solving multi-objective problems. Zhang *et al.* [26] proposed a MOPSO algorithm based on competition mechanism. The method is based on pairwise competition to update the particle swarm. The experimental results show that the

algorithm has well performance optimization quality and convergence speed. MOPSO has significant advantages compared to single-objective particle swarm optimization. This paper proposes to optimize the VMD parameters by using MOPSO, and apply the improved VMD algorithm to the gearbox composite fault diagnosis. The main part of the parameter optimization using this method is the selection of multi-objective functions. Because, SDE [27], [28] is from symbol dynamic filtering, combining the advantages of symbol dynamics and information theory, based on these advantages, it can effectively remove background noise, utilize state mode probability and state transition to retain fault information, SDE has better performance in vibration signal analysis of amplitude and frequency information. The SDE is similar to the definition of PE, but SDE is better than PE, which is mainly reflected in the better performance of SDE in the evaluation of time series amplitude difference, and SDE has the advantage of anti-noise. At the same time, considering the PSE [29] reflects the signal power varies with frequency, the PSE can effectively reflect the complexity of the signal frequency composition. When the sparseness of the signal is weak, the PSE value is large; when the signal exhibits strong sparsity, the PSE value is small. So, this paper chooses the SDE and PSE as the objective function of MOPSO. Then, the Pareto frontier optimal solution set is obtained by the MOPSO algorithm. Finally, the VMD parameter optimal combination (k, α) is obtained through normalization. The simulated signal and gearbox fault signal is analyzed using the improve VMD [30].

II. THEORETICAL FOUNDATION

A. VARIATIONAL MODAL DECOMPOSITION (VMD) ALGORITHM

VMD is a new approach to adaptive non-recursive signal decomposition. It uses iterative solution to the optimal solution of the variational model, and can adaptively separate the components to obtain the frequency center and bandwidth of each IMF. The overall framework is variational model problem. The decomposition process of complex signals using VMD is actually the solution process of the constructed variational function problem.

The VMD decomposes the original signal $x(t)$ into k limit-bandwidth IMFs, which can be expressed as:

$$u_k(t) = A_k(t) \cos(\varphi_k(t)) \quad (1)$$

where, $A_k(t)$ is the instantaneous amplitude of $u_k(t)$, and $w_k(t)$ is the instantaneous frequency of $u_k(t)$.

Using H^1 Gauss smoothness of the demodulated signal, the bandwidth of $u_k(t)$ is estimated, Finally, the constrained variational models of VMD algorithm are as follows: (2), (3).

$$\min_{(u_k)(\omega_k)} \left\{ \sum_k \left\| \partial_t \left[\sigma(t) + \frac{j}{t} u_t(t) \right] e^{-j\omega_k t} \right\|_2^2 \right\} \quad (2)$$

$$s.t \sum_k u_k = x(t) \quad (3)$$

where: ∂_t represents the partial derivative of t , and $\{u_k\} = \{u_1, \dots, u_k\}$ represents the k IMFs obtained by decomposing the signal $x(t)$. $\{w_k\} = \{w_1, \dots, w_k\}$ represents the center frequency of each IMF component.

In order to solve the optimal solution of the above variational model, the following form of Lagrange function is introduced here:

$$L(\{u_k\}, \{\omega_k\}, \lambda) = \alpha \sum_k \left\| \left[(\sigma(t) + \frac{j}{t}) \times u_k(t) \right] e^{-jw_k t} \right\|_2^2 + \left\| x(t) - \sum_k u_k(t) \right\|_2^2 + \left\langle \lambda(t), x(t) - \sum_k u_k(t) \right\rangle \quad (4)$$

where: λ is the Lagrange multiplier operator and α is the penalty factor.

Secondly, the time-frequency domain transform of equation (4) is performed, and the corresponding extremum solution is solved to obtain the frequency domain expression of the modal component u_k and the center frequency w_k :

$$u_k^{n+1}(w) = \frac{f(w) - \sum_{i=1, i \neq k}^k u_i(w) + \frac{\lambda(w)}{2}}{1 + 2} \alpha (w - w_k)^2 \quad (5)$$

$$w_k^{n+1} = \frac{\int_0^\infty w |u_k(w)|^2 dw}{\int_0^\infty |u_k(w)|^2 dw} \quad (6)$$

Finally, the Alternate Direction Method of Multipliers (ADMM) is used to solve the optimal solution of the constrained variational model. Thereby, the original signal $x(t)$ is decomposed into k IMFs. The specific steps of the algorithm are as follows:

- (1) The initialization of the parameters, set $\{u_k\}$, $\{w_k\}$, $\{\lambda^1\}$ and n to 0.
- (2) Update u_k^{n+1} , w_k^{n+1} according to equation (5) and (6).
- (3) Update the value of λ^{n+1} according to equation $\lambda^{n+1}(w) = \lambda^n(w) + \tau(f(w) - \sum_k^{n+1} u_k(w))$.
- (4) Until the equation $\sum_k \|u_k^{n+1} - u_k^n\|_2^2 / \|u_k^n\|_2^2 < \varepsilon$ is satisfied, the iteration is stopped and the loop is exited. Otherwise, the return step 2. Finally, k intrinsic mode functions can be obtained. Complete decomposition [31].

B. OPTIMIZATION OF VMD PARAMETERS BASED ON MULTI-OBJECTIVE PARTICLE SWARM OPTIMIZATION (MOPSO)

In the traditional VMD algorithm, due to the limitation of its algorithm theory, it is necessary to preset the number of decomposition modes k and the penalty factor α before performing signal processing. According to the theoretical study of the VMD, the preset decomposition modal number k is too large, there will be over-decomposition when processing the signal; If the k value is too small, the under-decomposition phenomenon will occur when the signal is

processed. If the value of the penalty factor α is larger, the smaller the bandwidth of the obtained k modal functions; the value of α is smaller, the larger the bandwidth of the obtained k modal functions. It can be seen that the preset k value and α value have great influence on the VMD decomposition result. Therefore, selecting the appropriate number of decomposition modes k and the penalty factor α are the key to accurately extract fault information. MOPSO is widely used because of its simple principle, fast convergence, and good global search performance. Therefore, this paper uses the MOPSO algorithm proposed by Coello *et al.* [21] to optimize the VMD parameters. The key part of optimizing the VMD parameters based on this algorithm is the selection of multiple fitness functions. Due to PSE is the extension of information entropy in the frequency domain, it is related to the distribution of frequency components. The frequency spectrum entropy is used to quantify the degree of the chaos of various fault vibration signals from the magnitude and distribution of frequency domain amplitude. PSE reflects the complexity of the signal frequency composition.

The principle of PSE algorithm is as follows:

Step1: Calculate the power spectrum of $x(t)$.

$$s(f) = \frac{1}{2\pi N} |x(w)|^2 \quad (7)$$

where N is the signal length; $x(w)$ is the Fourier transform of $x(t)$.

Step2: The probability density function of the spectrum is obtained by normalizing all frequency components:

$$P_i = \frac{s(f_i)}{\sum_{k=1}^N s(f_k)} \quad i = 1, 2, 3, 4, \dots, N \quad (8)$$

where $s(f_i)$ is the spectral energy of the frequency component f_i ; P_i is the corresponding probability density; N is the number of frequency components in the total probability density fast Fourier transform.

Step3: The PSE value is:

$$H = - \sum_{k=1}^N P_i \log P_i \quad (9)$$

Meanwhile, SDE combines the advantages of symbolic dynamics and information theory. It can effectively remove background noise, and use state mode probability and state transition to preserve fault information. SDE has well performance in vibration signal analysis of amplitude and frequency information [21].

The principle of the SDE algorithm is as follows:

Given a time series $X\{x(k), k = 1, 2, \dots, N\}$, the length is N , and the SDE algorithm steps are as follows:

Step1: Due to the advantages of adaptive segmentation, time series are converted to symbol time series (called symbolization).

Step2: Construct the embedded vector $Z_j^{m,\lambda}$ using symbol time series, the formula is as (10), (11).

$$Z_j^{m,\lambda} = \{z(j), z(j + \lambda), \dots, z(j + (m - 1)\lambda)\} \quad (10)$$

$$j = 1, 2, \dots, N - (m - 1)\lambda \quad (11)$$

where m represents the embedded size and λ represents the delay.

Step3: Calculate the probability $p(q_\alpha^{\varepsilon,m,\lambda})$ of each state pattern using equation (12).

The symbol time series in which the embedded size is m and the number of symbols is ε has ε^m state patterns.

$$p(q_\alpha^{\varepsilon,m,\lambda}) = \frac{\|\{j : j \leq N - (m - 1)\lambda, \text{type}(Z_j^{\varepsilon,m,\lambda}) = q_\alpha^{\varepsilon,m,\lambda}\}\|}{N - (m - 1)\lambda} \quad (12)$$

where $\text{type}(\cdot)$ represents the mapping of symbol space to state space. $\|\cdot\|$ indicates the cardinality of a set.

Step4: Construct the state mode matrix using the probability of state pattern $q_\alpha^{\varepsilon,m,\lambda}$ as

$$\left[p(q_1^{\varepsilon,m,\lambda}), p(q_2^{\varepsilon,m,\lambda}), \dots, p(q_m^{\varepsilon,m,\lambda}) \right]_{1 \times \varepsilon^m}$$

Step5: The state transition probability $p(\sigma_b | q_\alpha^{\varepsilon,m,\lambda})$ is calculated using the formula (13).

$$p(\sigma_b | q_\alpha^{\varepsilon,m,\lambda}) = \frac{\|\{j : j \leq N - m\lambda, \text{type}(Z_j^{\varepsilon,m,\lambda}) = q_\alpha^{\varepsilon,m,\lambda}, Z(j + m\lambda) = \sigma_b\}\|}{N - m\lambda} \quad (13)$$

where $\alpha = 1, 2, \dots, \varepsilon^m$; $b = 1, 2, \dots, \varepsilon$. ε represents the number of symbols; ε^m is the number of states.

Step6: The following (14) state transition matrix is constructed based on $p(\sigma_b | q_\alpha^{\varepsilon,m,\lambda})$:

$$\begin{bmatrix} p(\sigma_1 | q_1) & \dots & p(\sigma_\varepsilon | q_1) \\ \vdots & \ddots & \vdots \\ p(\sigma_1 | q_\varepsilon^m) & \dots & p(\sigma_\varepsilon | q_\varepsilon^m) \end{bmatrix}_{\varepsilon \times \varepsilon^m} \quad (14)$$

Step7: SDE based on Shannon entropy is calculated as follows:

$$SDE_{norm}(X, m, \lambda, \varepsilon) = - \sum_{\alpha=1}^{\varepsilon^m} p(q_\alpha^{\varepsilon,m,\lambda}) \ln p(q_\alpha^{\varepsilon,m,\lambda}) - \sum_{\alpha=1}^{\varepsilon^m} \sum_{b=1}^{\varepsilon} p(q_\alpha^{\varepsilon,m,\lambda}) \times \ln(p(q_\alpha^{\varepsilon,m,\lambda}) \cdot p(\sigma_b | q_\alpha^{\varepsilon,m,\lambda})) \quad (15)$$

Step8: The SDE value is normalized using the following formula.

$$SDE_{norm}(X, m, \lambda, \varepsilon) = SDE(X, m, \lambda, \varepsilon) / \ln(\varepsilon^{m+1}) \quad (16)$$

Therefore SDE satisfies that $0 < SDE_{norm}(X, m, \lambda, \varepsilon) < 1$

C. PARAMETER OPTIMIZATION STEPS ARE AS FOLLOWS

Step1: Set the basic parameters of the algorithm, including the population size np , the save set size nR , the maximum iteration number mI , the upper and lower bounds of each dimension position of a particle, Var Min and Var Max, the inertia weight W , and the learning factors c_1 and c_2 . Among them, when the number of populations is small, the algorithm is easy to fall into the local optimal possibility, affecting the global search ability. However, if the population is too large, it will increase the calculation time and affect the calculation efficiency. Therefore, when selecting the size of the population, the reliability and calculation time of the algorithm should be considered comprehensively. For a typical problem, it can be 30 populations, and for complex problems, it can be 50 populations. The algorithm uses 30 initial population numbers, each of which is equivalent to one vector. that is, 30 initial vectors are used in this algorithm; The save set size nR is to store all the non-dominated solution sets in the particle swarm into the save set. When the save set capacity reaches the maximum nR , the particles in the sparse area are preferentially retained when the save set is updated, and the particles in the dense area are replaced. And the global extremum is selected in the storage set, and the particle swarm continuously searches for the optimal solution under the guidance of the extreme value; The maximum number of iterations mI is a preset algorithm iteration stop condition. When the algorithm is iteratively updated to the corresponding number of times, the algorithm terminates; Var Min and Var Max can improve the global search ability of the particles and improve the convergence speed and convergence precision of the algorithm; The inertia weight W indicates how much the original velocity of the particle can be retained. In the process of algorithm iteration, the inertia weight value should be continuously reduced to ensure the strong global search ability of the algorithm. Therefore, this paper chooses the dynamic value of this parameter between 0.4 and 0.9; The learning factors c_1 and c_2 are also called acceleration constants, c_1 regulates the step size at which the particles fly to their best position, and c_2 regulates the step size at which the particles fly to the global best position.

Step2: Initialize the multi-objective particle swarm optimization parameter $[k, \alpha]$, randomly generate the position $P(i)$ of each particle, and initialize the velocity $V(i) = 0$ of each particle.

Step3: Calculate the fitness value of each particle in the population.

Where the value of PSE and the value of SDE are used to calculate the fitness value of each particle in the population. Because PSE and SDE are used as objective functions for parameter optimization, the values are used to measure the parameters. When the value of PSE is smaller, the signal exhibits strong sparse characteristics, and the IMF obtained by the VMD processing contains more fault characteristic information. The value of SDE is smaller, the more regular and periodic the distribution of time series, which can better

TABLE 1. The parameters of the simulation signal.

f_1	f_{n1}	f_{n2}	f_z	A_m	g	T_m	f_c
35Hz	15Hz	20Hz	135Hz	2	0.1	0.1	280Hz

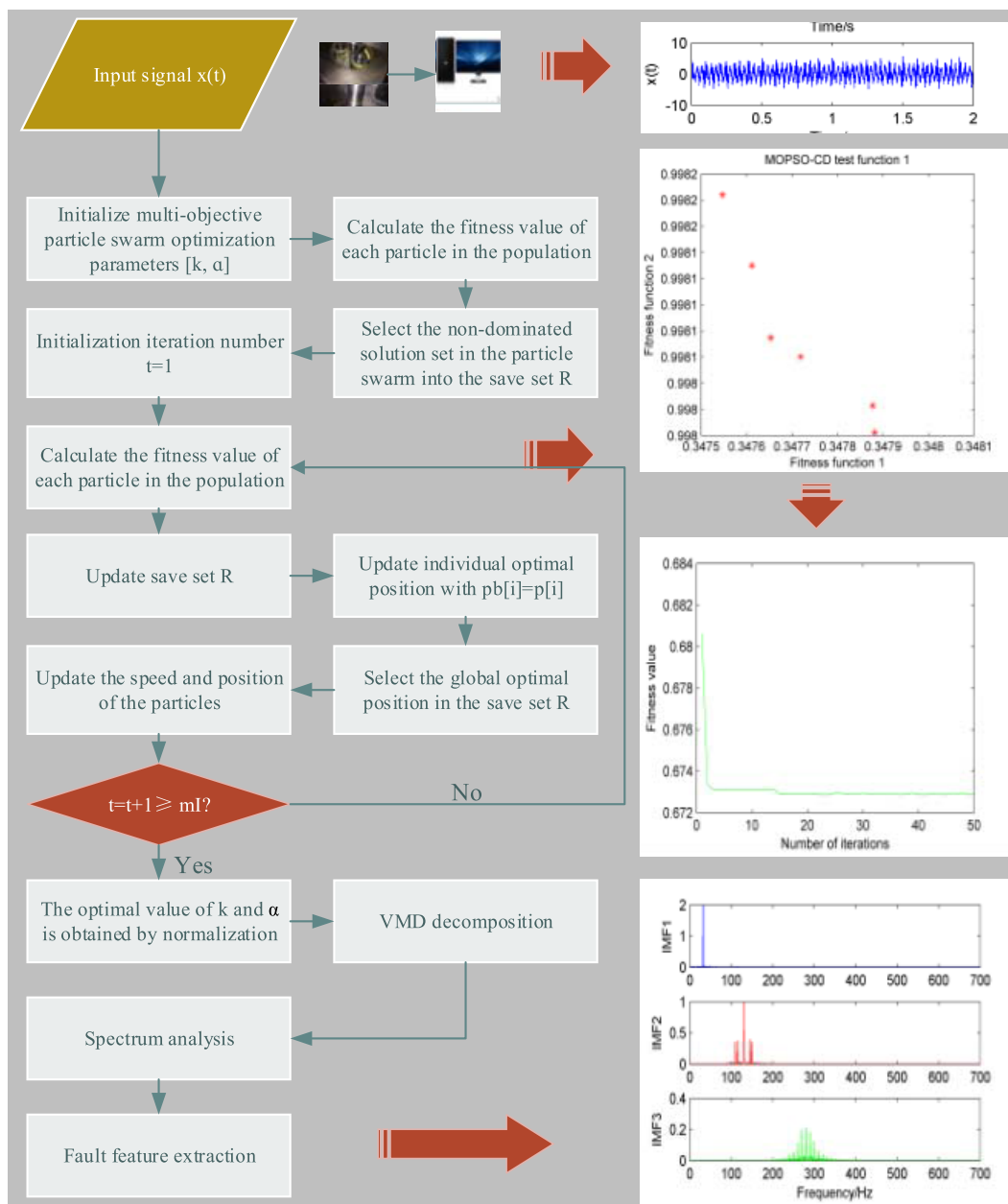


FIGURE 1. Flow chart of the proposed method.

measure the complexity of time series. Therefore, when the value of PSE and the value of SDEare small, the corresponding parameters are optimal.

Step4: Select the non-dominated solution from the particle swarm, and store them into save set R.

Step5: Generate a hypercubes for a search space, and locate the particles using hypercubes as a coordinate system. Which

defines the coordinates of each particle according to its objective function value.

Step6: Initialize the memory of each particle and store it in the save set R, which is also used as a guide to the search space.

Step7: Initialize the number of iterations $t = 1$, when the number of loop iterations is less than or equal to the maximum number of iterations mI , perform the following steps.

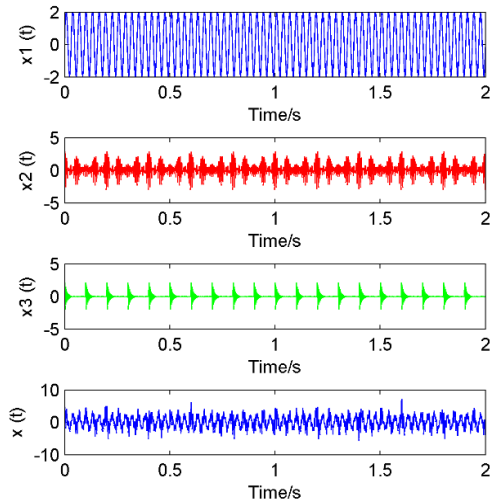


FIGURE 2. The time domain waveforms that make up the simulated signal.

a) Calculate each particle velocity using equation (17).

$$v(i) = w \times v[i] + c_1 \times r_1 \times (p_b[i] - p[i]) + c_2 \times r_2 \times (R[h] - p[i]) \quad (17)$$

where w is the inertia weight; c_1 and c_2 are the learning factors; r_1 and r_2 are the random numbers between $[0, 1]$; $p_b[i]$ is the historical optimal value of the particles; $p[i]$ is the current value of the particle i ; $R[h]$ is the value taken from the save set, and the index value h is selected as follows: first, divide any number $x > 1$ by the particle size, and the obtained value is assigned to a plurality of particle hypercube, Then, we apply roulette-wheel selection using these fitness values to select the hypercube from which we will take the corresponding particle. Once the hypercube has been selected, we select randomly a particle within such hypercube.

b) Update the new position of the particle as follows (18).

$$p[i] = p[i] + v[i] \quad (18)$$

c) Keep the particles in the search space to prevent them from crossing the border. When the decision variable exceeds the boundary, the decision variable first takes the corresponding boundary value, and then the flight speed is multiplied by (-1) to cause the particles to searches in the opposite direction.

d) Calculate the fitness value of each particle of the population.

e) Update save set R . Insert all current non-dominated solutions into the save set R , and the dominated solution will be deleted. Due to the capacity of the save set R is limited, once the capacity is maximized, the second criterion is applied, that is, the particles in the sparse area are preferentially retained, and the particles in the dense area are replaced.

f) When the current position of the particle is better than the individual historical optimal position, the particle position is updated with $P_b[i] = p[i]$. The Pareto dominance criterion is applied to determine which position in the memory is reserved. If the memory position dominates the current position, the memory position is retained; otherwise, the current position is retained. If neither is dominated by the other party, then choose one to make a reservation.

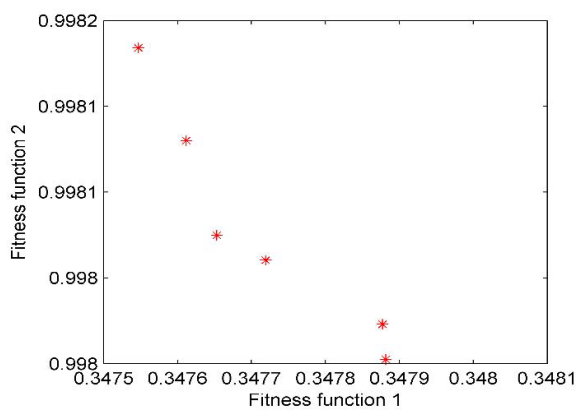
g) $t = t + 1$.

Step8: The number of cycles is equal to mI , ending the program.

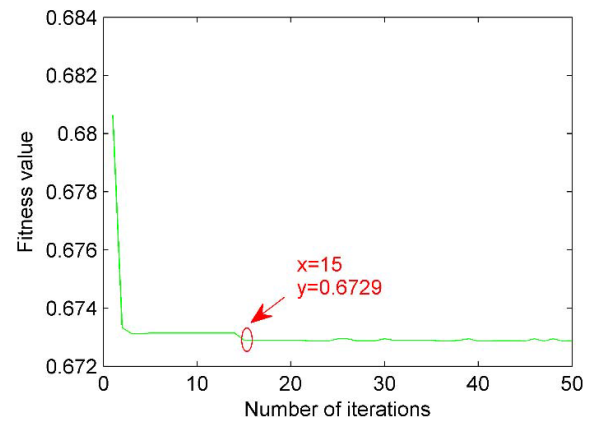
III. SIMULATION

A. SIMULATION SIGNAL CONSTRUCTION

When the gearbox has a composite fault, its vibration signal are often coexisting with multiple modulation sources. So, in order to make the simulation analysis closer to the engineering reality, the simulation signal should be closer to the actual gearbox fault signal. Therefore, in the construction of composite fault simulation signals, this paper uses the bearing



(a)



(b)

FIGURE 3. MOPSO (a) Pareto optimal frontier solution set; and (b) The fitness value during the iteration process.

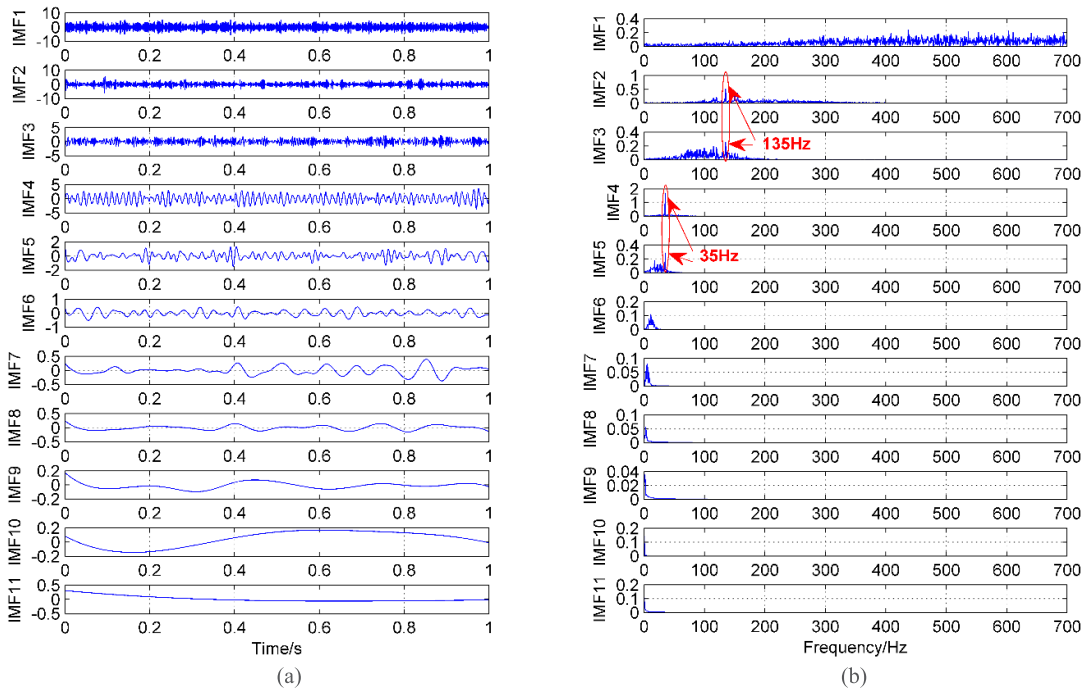


FIGURE 4. EEMD decomposed IMFs and their corresponding spectra. (a) Time domain of IMFs after EEMD; and (b) The spectrum corresponding to each layer of IMF.

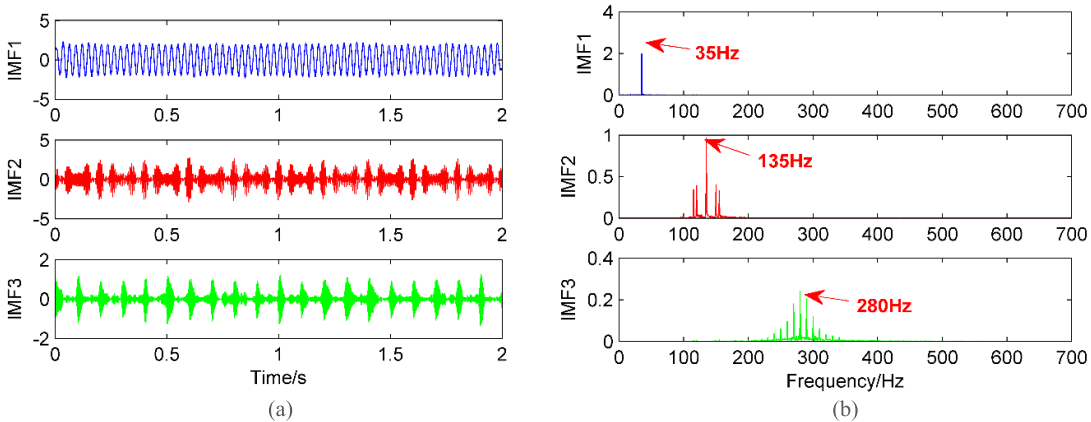


FIGURE 5. VMD decomposed IMFs and their corresponding spectra. (a) Time domain of IMFs after VMD; and (b) The spectrum corresponding to each layer of IMF.

inner ring fault signal and bearing rolling ball fault signal for simulation analysis. The composition of the simulation signal $x(t)$ is as shown in the following equation (19):

$$x(t) = x_1(t) + x_2(t) + x_3(t) + 2.5\text{randn}(t) \quad (19)$$

where: the composition signal $x_1(t) = 2 \sin(2\pi f_1 t)$ is a sinusoidal signal;

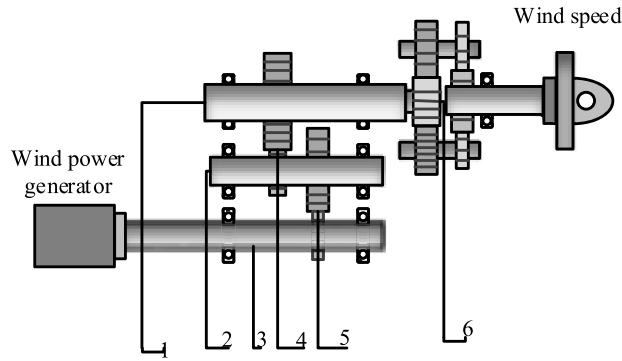
The composition signal $x_2(t) = (1 + \cos(2\pi f_{n1} t) + \cos(2\pi f_{n2} t)) \sin(2\pi f_z t)$ is a gear fault simulation signal with two modulation sources. f_{n1} and f_{n2} are the modulation

frequency of the modulation source and f_z is the carrier frequency, that is, the meshing frequency of the gear;

The composition signal $x_3(t) = A_m \times \exp(-g / -T_m) \sin(2\pi f_c t)$ is a periodic impact signal, which is specifically used to simulate the failure of the rolling bearing;

A_m represents the impact amplitude, g is the damping coefficient, T_m is the impact period, and f_c is the rotation frequency of the bearing;

The parameters of the simulated signal are shown in the following table 1:



1-intermediate shaft; 2-low speed shaft; 3-high speed shaft; 4-medium speed gear; 5-high speed gear; 6-planetary gear.

FIGURE 6. Wind turbine gearbox test bench.



FIGURE 7. Bearing inner ring and rolling element failure diagram. (a) Bearing inner ring peeling off; (b) bearing rolling body pitting.

Set the number of sampling points N to 3000 and the sampling frequency is 1500 Hz. The time-domain waveforms of the component signals $x_1(t)$, $x_2(t)$, $x_3(t)$, and the simulation signal $x(t)$ are shown in figure 2.

B. COMPARISON OF DIFFERENT ALGORITHM DECOMPOSITION RESULTS

The basic parameters of the multi-objective particle swarm optimization algorithm are set as follows [32].

The population size $np = 30$, the save set size $nR = 30$, the maximum iteration number $mI = 50$, the inertia weight $W = 0.5$, and the learning factor $c_1 = c_2 = 1.965$. By using the method proposed in this paper, the number of decomposition modal k and the penalty factor α in VMD are optimized, the Pareto frontier optimal solution set and the fitness value change with the number of iterations in the multi-objective particle swarm optimization process are shown in Figure 3. Among them, in figure 3(a), the fitness function 1 is the value of the symbol dynamic entropy (SDE) when calculating the fitness value of each particle in the population; The fitness function 2 is value of the power spectrum entropy (PSE) when calculating the fitness value of each particle in the population. In Figure 3(b), the fitness value is the average value of the symbol dynamic entropy value and the power spectrum entropy value. The minimum value in the iterative process is the best influence parameter value, duo

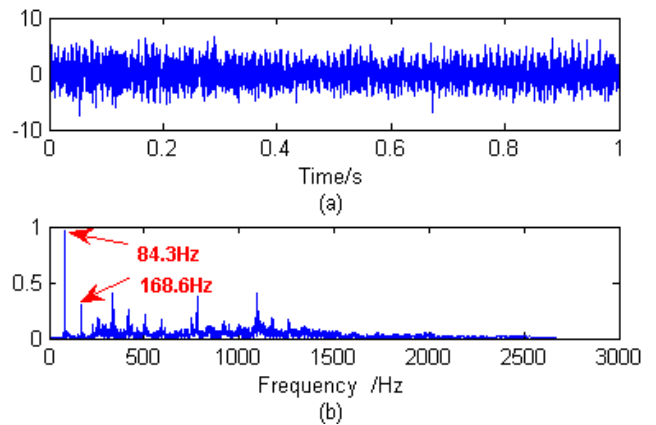


FIGURE 8. Time-frequency spectra of complex fault signal of gearbox. (a) Time domain of complex fault vibration signal; and (b) Spectrum of complex fault vibration signal.

to the PSE value is smaller, the signal exhibits strong sparse characteristics, and the IMF obtained by the VMD processing contains more fault characteristic information. The SDE value is smaller, the more regular and periodic the distribution of time series, which can better measure the complexity of time series. Therefore, when the smaller the mean value of the symbol dynamic entropy and the power spectrum entropy, corresponding parameters are optimal. That is, the optimal

TABLE 2. Failure frequency.

Intermediate shaft speed	Intermediate shaft frequency	Inner ring failure frequency	Rolling ball failure frequency
491.4rpm	8.19Hz	84.3Hz	27.3Hz

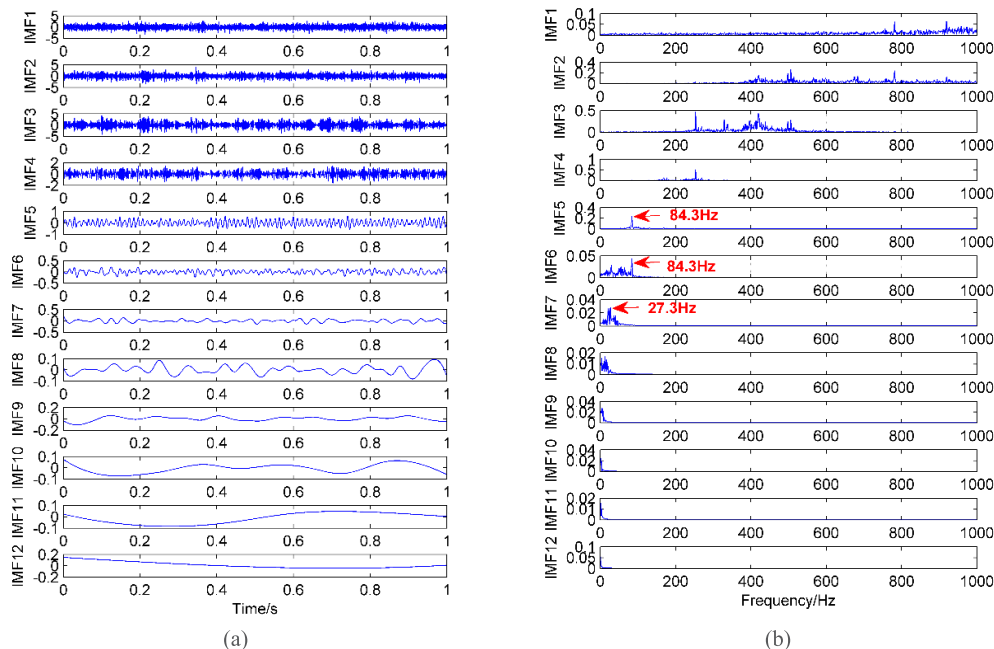


FIGURE 9. EEMD decomposed IMFs and their corresponding spectra. (a) Time domain of IMFs after EEMD; and (b) The spectrum corresponding to each layer of IMF.

impact parameter value is the minimum value during the iteration process.

Obviously, the minimum value of fitness value is 0.6729 with 15 iterations. The optimal impact parameter combination found is $[k, \alpha] = [3, 3548]$, and set the VMD algorithm parameter $k= 3, \alpha = 3548$. At the same time, the simulated signal is processed using the improved VMD algorithm.

In order to compare the results from different algorithms for the same simulation signals, this section will use EEMD and VMD to separately decompose the gearbox composite fault simulation signal $x_1(t)$ mentioned above. The analysis results are shown in figure 4 and figure 5.

It can be found in figure 4 that EEMD decomposes to 11 layers modal function when processing the simulated signal, but only the first five layers are meaningful. Among the decomposition results of EEMD, decomposed components are meaningless in IMF1; The frequency component of 130 Hz is decomposed into IMF2 and IMF3, and modal aliasing occurs. At the same time, the frequency component of 32 Hz is decomposed into IMF4 and IMF5, and modal aliasing also happens; The frequency component of 280 Hz in the original signal can't be extracted. It is shown that although EEMD adopts the idea of noise-assisted analysis,

it still cannot avoid the occurrence of modal aliasing. It can be found in figure 5, the VMD algorithm improved by the parameter optimization proposed in this paper decomposes to the 3 layers modal function when processing the simulation signal: the low frequency component of 32 Hz in the original signal is successfully extracted in IMF1, and its spectrum characteristics are very obvious; In IMF2, the 130 Hz center frequency of the amplitude modulated signal is successfully decomposed from the original signal containing strong noise; In IMF3, the center frequency of 280 Hz and the 10 Hz sideband uniformly distributed on both sides are also very obvious. Therefore, through comparing the decomposition results of the two algorithms, it is apparent that in the strong noise environment, the improved VMD can not only effectively eliminate the modal aliasing phenomenon of EEMD, but also obtain very obvious fault frequency characteristics.

IV. EXPERIMENTAL VERIFICATION

In order to verify the feasibility of the proposed method in engineering application, this method is applied to the composite fault diagnosis of wind power gearbox. The wind power gearbox test rig is used in this test verification, whose main components include: electric motor, wind power generator, the acceleration sensor, data acquisition analyzer,

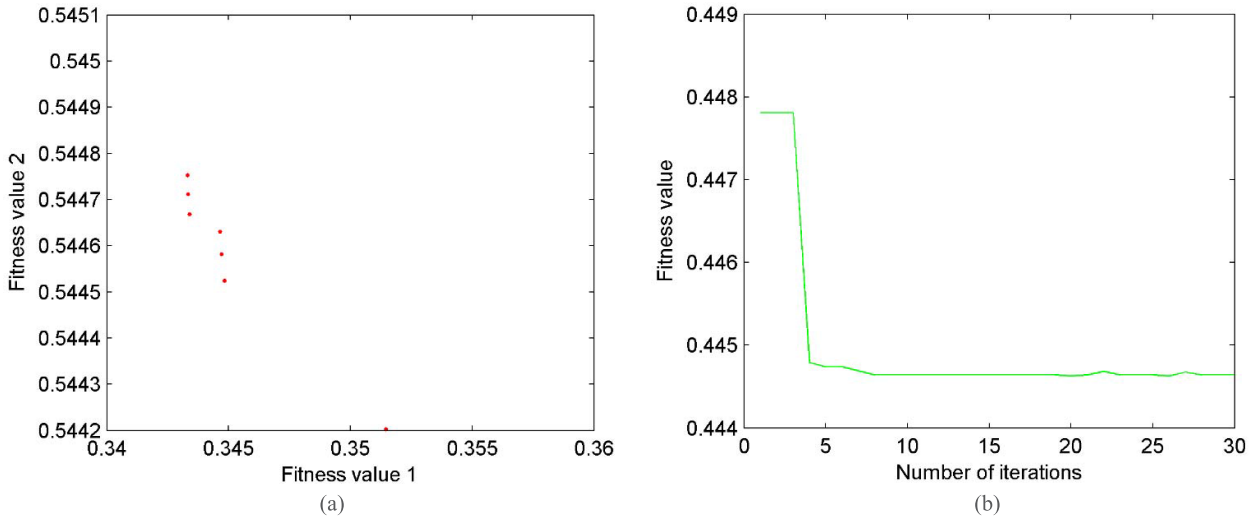


FIGURE 10. Multi-objective particle swarm optimization (a) Pareto optimal frontier solution set; and (b) The fitness value during the iteration process.

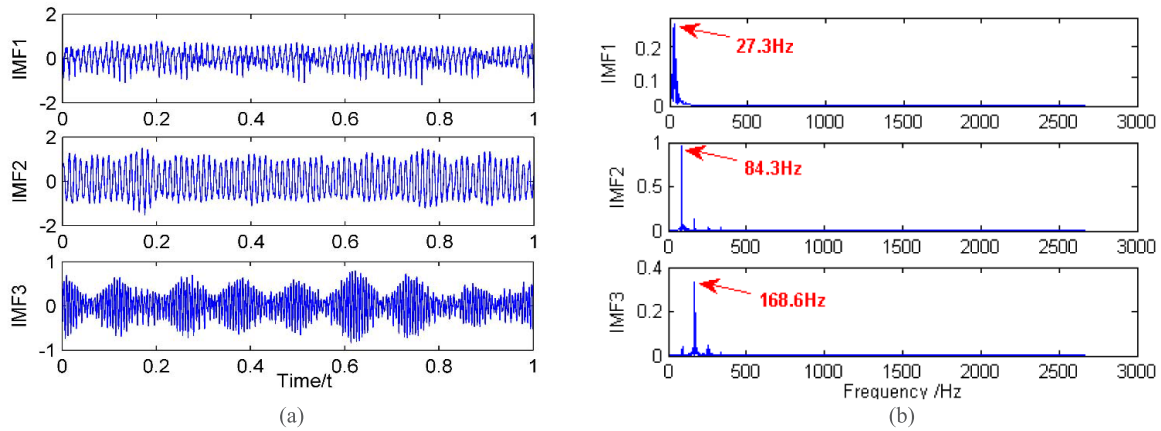


FIGURE 11. Time-spectrum diagram of IMFs after VMD decomposition. (a) Time domain of IMFs after VMD; and (b) The spectrum corresponding to each layer of IMF.

gearbox and so on. At the same time, the output shaft has a frequency of 30.24 Hz, the intermediate shaft frequency is 8.19 Hz, the low speed shaft frequency is 1.8 Hz, and the data sampling frequency is 5000 Hz. The fault frequency obtained by calculation is shown in table 2. The fault type of the gearbox in this experiment is a composite fault, which includes the inner ring of the bearing, as shown in figure 7(a); and the pitting of the bearing rolling ball, as shown in figure 7(b).

It can be seen from figure 8 that the periodic shock of the vibration signal collected by the sensor is irregular. However, in the frequency domain diagram obtained by the FFT transformation of the vibration signal, we can find the characteristic frequency of the inner ring fault 84.3 Hz and its double frequency 168.6 Hz, but there is no bearing rolling ball failure frequency 27.3 Hz does not appear. Thereby, the composite fault signal needs to be further decomposed.

A. EEMD DECOMPOSITION RESULTS OF FAULT SIGNALS

The vibration signal is analyzed by the EEMD method, and the obtained decomposition result is shown in figure 9.

As shown in the figure 9 that the signal is decomposed into 12 layers by the EEMD method, which the first four layers are noise components, and the 5th layer decomposes the bearing inner ring fault frequency 84.3 Hz. However, the 6th layer also decomposes the bearing inner ring fault frequency of 84.3 Hz, which occurs the mode aliasing phenomenon, the 7th layer decomposes the rolling ball fault frequency 27.3 Hz. 8th to 12th layer are meaningless interference components. It is obvious that the modal aliasing phenomenon occurs when the gearbox fault frequency is extracted by the EEMD method. Consequently, the fault frequency cannot be successfully extracted efficiently and accurately.

B. DECOMPOSITION RESULTS OF THE METHODS PROPOSED IN THIS PAPER

The vibration signal is analyzed by the method presented in this paper. Firstly, the power objective entropy (PSE) and symbol dynamic entropy (SDE) are used as the fitness function to calculate the fitness value. Then the Pareto frontier

optimal solution set is determined using the multi-objective particle swarm optimization algorithm through iteration. The minimum value of the fitness obtained after processing is 0.444, The optimal combination of parameters found is $[k, \alpha] = [3, 4000]$, as shown in Figure 10. The fault signal of the gearbox is decomposed by the VMD decomposition method after parameter optimization, and the result is shown in figure 11. The spectrogram of figure 11 shows that the rolling ball fault frequency of 27.3 Hz and the inner ring fault frequency of 84.3 Hz in the gearbox fault signal are successfully extracted. Meanwhile, IMF3 decomposes out the double frequency 168.6 Hz of the inner ring fault frequency 84.3 Hz, and the spectral characteristics are very obvious. Compared to EEMD decomposition, VMD decomposition doesn't emerge modal aliasing. The validity of the proposed method is proved.

V. CONCLUSION

This paper proposes a method to improve the VMD parameters and successfully applied to the fault diagnosis of wind power gearbox. The proposed method can efficiently and accurately determine the VMD parameter combination (k, α) , as well as effectively extract the composite fault characteristics in the gearbox. The effectiveness of the proposed method is verified by simulation and experiment.

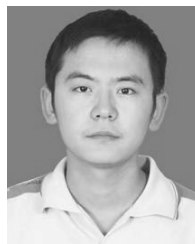
The PSE and SDE proposed in this paper are fitness functions, and then multi-objective particle swarm optimization algorithm is used to obtain the Pareto frontier optimal solution set, followed by normalization to get the optimal combination of VMD parameters (k, α) . The VMD algorithm with these adaptive parameters of the optimization algorithm not only overcomes the limitations of the VMD but also successfully extracts the composite fault characteristics of the gearbox under a strong background noise environment. And the validity of the algorithm is confirmed.

Compared with EEMD, the VMD decomposition signal with optimized parameters does not exhibit modal aliasing.

REFERENCES

- [1] B. Cai et al., "Multi-source information fusion based fault diagnosis of ground-source heat pump using Bayesian network," *Appl. Energy*, vol. 114, pp. 1–9, Feb. 2014. doi: [10.1016/j.apenergy.2013.09.043](https://doi.org/10.1016/j.apenergy.2013.09.043).
- [2] B. Cai, Y. Zhao, H. Liu, and M. Xie, "A data-driven fault diagnosis methodology in three-phase inverters for PMSM drive systems," *IEEE Trans. Power Electron.*, vol. 32, no. 7, pp. 5590–5600, Jul. 2017. doi: [10.1109/TPEL.2016.2608842](https://doi.org/10.1109/TPEL.2016.2608842).
- [3] B. Cai, Y. Liu, Y. Ma, Z. Liu, Y. M. Zhou, and J. Sun, "Real-time reliability evaluation methodology based on dynamic Bayesian networks: A case study of a subsea pipe ram BOP system," *ISA Trans.*, vol. 58, pp. 595–604, Sep. 2015. doi: [10.1016/j.isatra.2015.06.011](https://doi.org/10.1016/j.isatra.2015.06.011).
- [4] B. Cai, Y. Liu, Z. Liu, X. Tian, Y. Zhang, and R. Ji, "Application of Bayesian networks in quantitative risk assessment of subsea blowout preventer operations," *Risk Anal.*, vol. 33, no. 7, pp. 1293–1311, Jul. 2013. doi: [10.1111/j.1539-6924.2012.01918.x](https://doi.org/10.1111/j.1539-6924.2012.01918.x).
- [5] K. Dragomiretskiy and D. Zosso, "Variational mode decomposition," *IEEE Trans. Signal Process.*, vol. 62, no. 3, pp. 531–544, Feb. 2014. doi: [10.1109/TSP.2013.2288675](https://doi.org/10.1109/TSP.2013.2288675).
- [6] X. An, Y. Tian, and H. Zeng, "Vibration signal analysis of a hydropower unit based on noise-assisted multivariate empirical mode decomposition," *Int. J. Acoust. Vib.*, vol. 23, no. 4, pp. 448–453, Dec. 2018. doi: [10.20855/ijav.2018.23.41129](https://doi.org/10.20855/ijav.2018.23.41129).
- [7] M. S. Hoseinzadeh, S. E. Khadem, and M. S. Sadooghi, "Quantitative diagnosis for bearing faults by improving ensemble empirical mode decomposition," *ISA Trans.*, vol. 83, pp. 261–275, Dec. 2018. doi: [10.1016/j.isatra.2018.09.008](https://doi.org/10.1016/j.isatra.2018.09.008).
- [8] F. Jiang, Z. Zhu, W. Li, S. Xia, and G. Zhou, "Lifting load monitoring of mine hoist through vibration signal analysis with variational mode decomposition," *J. Vibroeng.*, vol. 19, no. 8, pp. 6021–6035, Dec. 2017. doi: [10.21595/jve.2017.18859](https://doi.org/10.21595/jve.2017.18859).
- [9] Z. Li, Y. Jiang, C. Hu, and Z. Peng, "Difference equation based empirical mode decomposition with application to separation enhancement of multi-fault vibration signals," *J. Difference Equ. Appl.*, vol. 23, nos. 1–2, pp. 457–467, Feb. 2017. doi: [10.1080/10236198.2016.1254206](https://doi.org/10.1080/10236198.2016.1254206).
- [10] Z. Wang et al., "Research and application of improved adaptive MOMEDA fault diagnosis method," *Measurement*, vol. 140, pp. 63–75, Jul. 2019. doi: [10.1016/j.measurement.2019.03.033](https://doi.org/10.1016/j.measurement.2019.03.033).
- [11] H. Wang, P. Wang, L. Song, B. Ren, and L. Cui, "A novel feature enhancement method based on improved constraint model of online dictionary learning," *IEEE Access*, vol. 7, pp. 17599–17607, Jan. 2019. doi: [10.1109/ACCESS.2019.2895776](https://doi.org/10.1109/ACCESS.2019.2895776).
- [12] L. Song, H. Wang, and P. Chen, "Step-by-step fuzzy diagnosis method for equipment based on symptom extraction and trivalent logic fuzzy diagnosis theory," *IEEE Trans. Fuzzy Syst.*, vol. 26, no. 6, pp. 3467–3478, Dec. 2018. doi: [10.1109/TFUZZ.2018.2833820](https://doi.org/10.1109/TFUZZ.2018.2833820).
- [13] Z. Wang et al., "A novel fault diagnosis method of gearbox based on maximum kurtosis spectral entropy deconvolution," *IEEE Access*, to be published. doi: [10.1109/ACCESS.2019.2900503](https://doi.org/10.1109/ACCESS.2019.2900503).
- [14] H. Cao, Y. Zhang, C. Shen, Y. Liu, and X. Wang, "Temperature energy influence compensation for MEMS vibration gyroscope based on RBF NN-GA-KF method," *Shock Vib.*, vol. 2018, Dec. 2018, Art. no. 2830686. doi: [10.1155/2018/2830686](https://doi.org/10.1155/2018/2830686).
- [15] X. Zhang, Q. Miao, H. Zhang, and L. Wang, "A parameter-adaptive VMD method based on grasshopper optimization algorithm to analyze vibration signals from rotating machinery," *Mech. Syst. Signal Process.*, vol. 108, pp. 58–72, Aug. 2018. doi: [10.1016/j.ymsp.2017.11.029](https://doi.org/10.1016/j.ymsp.2017.11.029).
- [16] Z. Wang, J. Wang, and W. Du, "Research on fault diagnosis of gearbox with improved variational mode decomposition," *Sensors*, vol. 18, no. 10, p. 3510, Oct. 2018. doi: [10.3390/s18103510](https://doi.org/10.3390/s18103510).
- [17] M. Yonghao, Z. Ming, and L. Jing, "Identification of mechanical compound-fault based on the improved parameter-adaptive variational mode decomposition," *ISA Trans.*, vol. 84, pp. 82–95, Jan. 2019. doi: [10.1016/j.isatra.2018.10.008](https://doi.org/10.1016/j.isatra.2018.10.008).
- [18] Y. Zhou, H. E. Fazhi, and Y. Qiu, "Dynamic strategy based parallel ant colony optimization on GPUs for TSPs," *Sci. China Inf. Sci.*, vol. 60, no. 6, Jun. 2017, Art. no. 068102. doi: [10.1007/s11432-015-0594-2](https://doi.org/10.1007/s11432-015-0594-2).
- [19] W. Shen, X. Guo, C. Wu, and D. Wu, "Forecasting stock indices using radial basis function neural networks optimized by artificial fish swarm algorithm," *Knowl.-Based Syst.*, vol. 24, no. 3, pp. 378–385, 2011. doi: [10.1016/j.knsys.2010.11.001](https://doi.org/10.1016/j.knsys.2010.11.001).
- [20] C. Ding, M. Zhao, J. Lin, and J. Jiao, "Multi-objective iterative optimization algorithm based optimal wavelet filter selection for multi-fault diagnosis of rolling element bearings," *ISA Trans.*, Dec. 2018. doi: [10.1016/j.isatra.2018.12.010](https://doi.org/10.1016/j.isatra.2018.12.010).
- [21] C. A. C. Coello, G. T. Pulido, and M. S. Lechuga, "Handling multiple objectives with particle swarm optimization," *IEEE Trans. Evol. Comput.*, vol. 8, no. 3, pp. 256–279, Jun. 2004. doi: [10.1109/TEVC.2004.826067](https://doi.org/10.1109/TEVC.2004.826067).
- [22] Q. Lin, J. Li, Z. Du, J. Chen, and Z. Ming, "A novel multi-objective particle swarm optimization with multiple search strategies," *Eur. J. Oper. Res.*, vol. 247, no. 3, pp. 732–744, Dec. 2015. doi: [10.1016/j.ejor.2015.06.071](https://doi.org/10.1016/j.ejor.2015.06.071).
- [23] M. S. Hasanoglu and M. Dolen, "Multi-objective feasibility enhanced particle swarm optimization," *Eng. Optim.*, vol. 50, no. 12, pp. 2013–2037, Dec. 2018. doi: [10.1080/0305215X.2018.1431232](https://doi.org/10.1080/0305215X.2018.1431232).
- [24] C. Gong, H. Chen, W. He, and Z. Zhang, "Improved multi-objective clustering algorithm using particle swarm optimization," *PLoS ONE*, vol. 12, no. 12, Dec. 2017, Art. no. e0188815. doi: [10.1371/journal.pone.0188815](https://doi.org/10.1371/journal.pone.0188815).
- [25] S. S.-K. Fan, J.-M. Chang, and Y.-C. Chuang, "A new multi-objective particle swarm optimizer using empirical movement and diversified search strategies," *Optim. Eng.*, vol. 47, no. 6, pp. 750–770, Jun. 2015. doi: [10.1080/0305215X.2014.918116](https://doi.org/10.1080/0305215X.2014.918116).
- [26] X. Zhang, X. Zheng, R. Cheng, J. Qiu, and Y. Jin, "A competitive mechanism based multi-objective particle swarm optimizer with fast convergence," *Inf. Sci.*, vol. 427, pp. 63–76, Feb. 2018. doi: [10.1016/j.ins.2017.10.037](https://doi.org/10.1016/j.ins.2017.10.037).

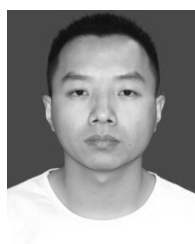
- [27] Y. Li, Y. Yang, G. Li, M. Xu, and W. Huang, "A fault diagnosis scheme for planetary gearboxes using modified multi-scale symbolic dynamic entropy and mRMR feature selection," *Mech. Syst. Signal Process.*, vol. 91, pp. 295–312, Jul. 2017. doi: [10.1016/j.ymssp.2016.12.040](https://doi.org/10.1016/j.ymssp.2016.12.040).
- [28] Y. Li, Y. Yang, X. Wang, B. Liu, and X. Liang, "Early fault diagnosis of rolling bearings based on hierarchical symbol dynamic entropy and binary tree support vector machine," *J. Sound Vib.*, vol. 428, pp. 72–86, Aug. 2018. doi: [10.1016/j.jsv.2018.04.036](https://doi.org/10.1016/j.jsv.2018.04.036).
- [29] Y. Ji et al., "EEMD-based online milling chatter detection by fractal dimension and power spectral entropy," *Int. J. Adv. Manuf. Technol.*, vol. 92, nos. 1–4, pp. 1185–1200, Sep. 2017. doi: [10.1007/s00170-017-0183-7](https://doi.org/10.1007/s00170-017-0183-7).
- [30] Y. Li, G. Cheng, C. Liu, and X. Chen, "Study on planetary gear fault diagnosis based on variational mode decomposition and deep neural Networks," *Measurement*, vol. 130, pp. 94–104, Dec. 2018. doi: [10.1016/j.measurement.2018.08.002](https://doi.org/10.1016/j.measurement.2018.08.002).
- [31] A. Venkitaraman, S. Chatterjee, and P. Händel, "On Hilbert transform, analytic signal, and modulation analysis for signals over graphs," *Signal Process.*, vol. 156, pp. 106–115, Mar. 2019. doi: [10.1016/j.sigpro.2018.10.016](https://doi.org/10.1016/j.sigpro.2018.10.016).
- [32] A. R. Jordehi and J. Jasni, "Parameter selection in particle swarm optimisation: A survey," *J. Exp. Theor. Artif. Intell.*, vol. 25, no. 4, pp. 527–542, Dec. 2013. doi: [10.1080/0952813X.2013.782348](https://doi.org/10.1080/0952813X.2013.782348).



XIAOFENG HAN received the B.S. degree from the North University of China, where he is currently pursuing the master's degree. His research interests are mainly in the areas of research on fault diagnosis of gearbox. He has published a research paper in scholarly journal in the above research area.



JINGTAI WANG received the bachelor's degree in engineering from the College of Information and Business, North University of China, where he is currently pursuing the master's degree. His research interests are mainly in the areas of mechanical fault diagnosis and signal processing.



HUIHUI HE received the degree from the Changsha Aviation Vocational and Technical College, in 2013, with a major in mechanical and electrical integration. He is currently pursuing the master's postgraduate with the School of Mechanical Engineering, North University of China. His main research areas include the composite fault diagnosis of rotating machinery gearbox.



XIAOMING GUO received the bachelor's degree from the North University of China, where he is currently pursuing the master's degree in mechanical engineering. His research interests are mainly in the areas of fault diagnosis of rotating machinery.



JUNYUAN WANG received the Ph.D. degree from the Taiyuan University of Technology. He is currently a Professor with the North University of China, the Vice Chairman of the Shanxi Province Society of Vibration Engineering, the Executive Director and Deputy Secretary-General of the Shanxi Province Mechanical Engineering Society, and the Vice Chairman of the Mechanical Transmission Branch of the Shanxi Province Mechanical Engineering Society. His research interests include intelligent manufacturing technology and system.



YANFEI KOU received the Ph.D. degree in mechanical engineering from the Taiyuan University of Technology, Taiyuan, China. He has published over ten academic papers. His main research interests include coal mining machinery.

...



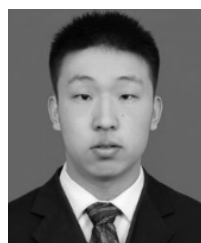
ZHIJIAN WANG received the Ph.D. degree from the Taiyuan University of Technology, Taiyuan, China. He is currently an Associate Professor with North China University. His research interests include mechanical fault diagnosis, signal processing, and intelligent diagnosis. He has published over a dozen papers in these fields. He is a member of the Chinese Society of Vibration Engineering.



GAOFENG HE received the B.S. degree from the College of Information and Business, North University of China, where he is currently pursuing the master's degree. His research interests are mainly in the areas of research on fault diagnosis of gearbox.



WENHUA DU received the Ph.D. degree from Tianjin University, Tianjin, China. She was a Visiting Scholar with Warwick University, from 2016 to 2017. She is currently a Professor with North China University. Her research interests include mechanical dynamics and machine vision.



JIE ZHOU received the bachelor's degree from Xi'an Technological University, Xian, China, in 2016. He is currently pursuing the master's postgraduate with the School of Mechanical Engineering, North University of China, Shanxi, China. His research interests include mechanical fault diagnosis and signal processing.